TÜBİTAK

Turkish Journal of Chemistry

http://journals.tubitak.gov.tr/chem/

Research Article

Turk J Chem
(2015) 39: 532 – 549

doi:10.3906/kim-1412-13

Two new coordination polymers containing dicyanidoargentate(I) and dicyanidoaurate(I): synthesis and characterization, and a detailed in vitro investigation of their anticancer activities on some cancer cell lines

Ali AYDIN[1,*], Ahmet KARADAĞ[2], Şaban TEKİN[1], Nesrin KORKMAZ[2], Aslıhan ÖZDEMİR[2]

[1]Department of Molecular Biology, Science and Arts Faculty, Gaziosmanpaşa University, Tokat, Turkey
[2]Department of Chemistry, Science and Arts Faculty, Gaziosmanpaşa University, Tokat, Turkey

Received: 06.12.2014 • **Accepted/Published Online:** 16.02.2015 • **Printed:** 30.06.2015

Abstract: Two novel cyanido-bridged bimetallic polymeric complexes, $[Ni(edbea)Ag_3(CN)_5]_n$ (***C1***) and $[Ni(bishydeten)Au_2(CN)_4]_n$ (***C2***), where e*dbea* = [2,2′-(ethylenedioxy)bis(ethylamine)] and *bishydeten* = [(*N*,*N*′-bis(2-hydroxyethyl) ethylenediamine)] are ligands, were synthesized and characterized by elemental, infrared, and thermal measurement techniques and investigated for their biological activity in cultured cancer cell lines. The results show that both compounds and free anions, $[Ag(CN)_2]^-$ and $[Au(CN)_2]^-$, exhibited very high antiproliferative activity compared to the anticancer drug 5FU against the cancer cell lines tested. The antiproliferative and cytotoxic activities of ***C1*** and ***C2*** were significantly lower than those of free anions, indicating that the extreme cytotoxicity of free anions decreased to safe levels in ***C1*** and ***C2***. In conclusion, the results show that these novel compounds possess anticancer activities.

Key words: Dicyanidoargentate(I), dicyanidoaurate(I), coordination polymers, anticancer activity, apoptosis

1. Introduction

The use of metals in medicine dates back to antiquity, with various complexes being used to treat different ailments. Even today, metal complexes and their application in medicine have been studied extensively.[1,2] The use of metal complexes as a chemotherapeutic agent in the treatment of cancer may lead to alternatives to the anticancer agents presently being used.[3,4]

From this perspective, Kelland et al.[5] reported the first metal-based anticancer drug, cisplatin, which is used in the treatment of ovarian cancer. Metal complexes such as silver, gold, and platinum are metabolized in the body to form complexes with the amino and carboxyl groups in RNA, DNA, and proteins. For example, the platinum center in cisplatin is known to coordinate DNA, thereby disrupting DNA replication. In recent years, silver and gold complexes have been reported to have anticancer activity in vitro.[6] Various silver and gold compounds with interesting antitumor activity have been reported. For example, Zachariadis et al.[7] found that Ag(I) complexes of heterocyclic thioamide 2-mercapto-3,4,5,6-tetrahydropyrimidine derivatives possess anticancer activity against certain types of cancer. El-din et al.[8] reported $[SnMe_3(bpe)][Ag(CN)_2].2H_2O$, where bpe is 1,2-bis(4-pyridyl)ethane and $SnMe_3$ is a ligand that possesses anticancer activity against human carcinoma cells. Liu et al.[9] showed that Au(I) and Ag(I) bidendate pyridyl phosphine complexes possess

*Correspondence: aliaydin.bio@gmail.com

anticancer activity against cisplatin-resistant human cancer cells (CH1-cisR, 41M-cisR, and SKOV-3) based on their lipophilicity. Moreover, Au(III) compounds possess certain promising anticancer activities, as observed by Sun et al.[10]

Many anticancer drugs kill normal growing cells together with cancerous cells. This damage to normal cells causes side effects. Hence, the major drawback of using old anticancer agents is adverse effects such as nausea, bone marrow suppression, and kidney toxicity, which are experienced by patients receiving chemotherapy.[11] Another major drawback of old anticancer agents is the drug resistance that usually occurs.[11] There are various types of cancers that are inherently resistant to anticancer agents, with drugs having no effect. Therefore, there is a need for new approaches to address these drawbacks.

Research efforts are focused on developing novel antitumor drugs to ameliorate clinical effectiveness and to minimize general toxicity and drug resistance.[12] Silver and gold complexes are found to be promising alternatives to old anticancer agents, showing activity on tumors that have developed resistance.[13] The serious limitations of cancer treatments have prompted many researchers to develop alternative strategies based on different metals, ligands, and mechanisms for cancer.[14] Transition metal complexes of this type have not been extensively explored for their chemotherapeutic usage.

This paper shows a new class of silver and gold complexes denoted as ***C1*** and ***C2***, which were tested for their anticancer activity against rat glioma (C6), human cervical cancer (HeLa), human colon cancer (HT29), and African green monkey kidney (Vero) cell lines. In the present study, the use of different N- and $O-$donor ligands, *edbea* [2,2′-(ethylenedioxy)bis(ethylamine)] and *bishydeten* [(N,N'-bis(2-hydroxyethyl) ethylenediamine)], led to various types of structures and different function of the cyanido groups (e.g., terminal or bridging), reflected by the ν(CN) stretching vibration positions in the IR spectra of ***C1*** and ***C2***. Dicyanidoargentate(I) $\{[Ag(CN)_2]^-\}$ and dicyanidoaurate(I) $\{[Au(CN)_2]^-\}$ are linear anions with considerable stability and simplicity. These were used to successfully synthesize $[Ni(edbea)Ag_3(CN)_5]_n$ (***C1***) and $[Ni(bishydeten)Au_2(CN)_4]_n$ (***C2***). Free $[Ag(CN)_2]^-$ and $[Au(CN)_2]^-$ are known to be highly cytotoxic. The newly synthesized silver and gold complexes containing $[Ag(CN)_2]^-$ and $[Au(CN)_2]^-$ have anticancer properties but low cytotoxicity.

2. Results and discussion

2.1. Results

2.1.1. Structural description

X-ray single crystal analyses of ***C1*** and ***C2*** could not be performed as it was not possible to obtain suitable crystals. ***C1*** and ***C2*** obtained as powder crystals are well soluble in DMSO and much less soluble in water. Recrystallization in DMSO of the complexes is not possible due to its donor character. Furthermore, recrystallization of the complexes in different solvents was not possible. Therefore, the characterization of the complexes was conducted using some other techniques. The molecular structures of ***C1*** and ***C2*** were estimated by taking advantage of the literature[15–20] related to *edbea* and *bishydeten* ligands and using elemental, IR, and thermal measurements. The neutral ligands *edbea* and *bishydeten* were observed to act as two, three, or four dentate in our previous studies[15–20] and it is known that the ligands behave as either two or three dentate in the polymeric structure. On the other hand, thermal analysis data provide quite remarkable results about the structures of the complexes. For example, thermal stability can be seen as an important criterion in the structural description. Moreover, the exchange of cyanido stretching vibration peak values and numbers are important for the structural definition of the complexes. ***C1*** and ***C2*** were formulated as $[Ni(edbea)Ag_3(CN)_5]$n

and [Ni(*bishydeten*)$Au_2(CN)_4$]n, respectively, considering the results of elemental and thermal analysis. Hereby, the molecular structures of ***C1*** and ***C2*** by taking into consideration IR, elemental, thermal analysis, and literature data might be depicted as in the Scheme.

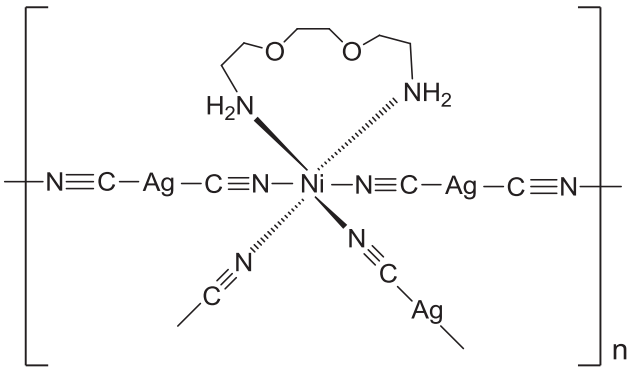

C1

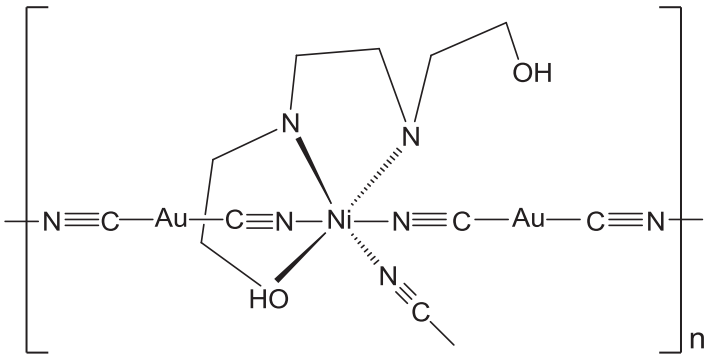

C2

Scheme

2.1.2. Fourier transform-infrared spectra (FT-IR)

Cyanido complexes are easily identifiable owing to sharp cyanido stretching vibration peaks at 2200–2000 cm^{-1}.[21] Characteristic cyanido stretching vibration peaks of ***C1*** and ***C2*** (peak at 2161 cm^{-1} and peaks at 2194, 2173, and 2150 cm^{-1}, respectively) were observed at higher frequencies than those belonging to $K[Ag(CN)_2]$ (2136 cm^{-1}) and $K[Au(CN)_2]$ (2140 cm^{-1}) complexes. This suggests ***C1*** could be a complex in which all cyanide groups behaved as a bridge because there is only one strong single cyanido peak at 2150 cm^{-1}. Moreover, the three cyanido peaks observed at 2194, 2173, and 2150 cm^{-1} for ***C2*** indicate the presence of both terminal and bridging cyanido groups.

Other prominent peaks in the IR spectra of ***C1*** and ***C2*** are the stretching vibration peaks belonging to the NH_2, CH_2, and CO groups of neutral *edbea* ligand and the OH, NH_2, and CH_2 groups of neutral *bishydeten* ligand.[15–20] Four peaks at 2906 and 2865 cm^{-1} with 1101 and 1031 cm^{-1} were attributed to $–CH_2$ and –CO groups, respectively, while $–NH_2$ stretching vibrations of *edbea* were observed at 3342 and 3276 cm^{-1}. On the other hand, the ν(OH), ν(NH), and ν(CH) vibrational frequencies of *bishydeten* appeared at 3446, 3255 and 3220, and 2938 and 2881 wave numbers, respectively.

2.1.3. Thermal analyses

The thermal stability and decomposition behavior of ***C1*** and ***C2*** were studied by thermogravimetry-differential thermal analysis (TG-DTA) in flowing atmosphere of N_2. The general way of the thermal decomposition of cyanido complexes is characterized by leaving of N-donor ligands and then decomposition of all cyanido groups in one step.[22–24] Thermal decompositions of ***C1*** and ***C2*** are three- to four-stage processes. Moreover, DTA curves show that the complexes have no melting points. Thermal analysis data for ***C1*** and ***C2*** are given in Table 1.

Table 1. Thermoanalytical data for ***C1*** and ***C2***.

Complex	Stage	Temperature range (°C)	DTG_{max} (°C)	Mass loss, Δm (%)		Total mass loss, Δm (%)		Removed group
				Found.	Calc.	Found.	Calc.	
$C_{11}H_{16}N_7O_2Ag_3Ni$ (***C1***) MA: 660.59	1	140–338	305	8.33	22.44	8.33	22.44	*edbea*
	2	338–455	397	14.85		23.18		
	3	455–982	952	19.81	19.69	42.99	42.13	5CN
$C_{10}H_{16}N_6O_2NiAu_2$ (***C2***) MA:704.90	1	221–308	263	16.17	33.52	16.17	33.52	*bishydeten* 4CN
	2	308–418	378	10.54		26.71		
	3	418–486	452	4.11		30.82		
	4	486–570	510	2.73		33.55		

The first process in the thermal decomposition of ***C1*** is the release of *edbea* in the 140–338 °C temperature range with an endothermic process (found 23.18% calc. 22.44%). The observed total weight loss of 19.81% corresponds to the liberation of all five cyanido molecules in the 455–982 °C temperature range (calc. 19.69%). The most probable thermal decomposition scheme of ***C1*** is given below:

$$[Ni(edbea)Ag_3(CN)_5] \xrightarrow[-edbea]{140-455^\circ C} [NiAg_3(CN)_5] \xrightarrow[-5CN]{445-982^\circ C} Ni + 3Ag$$

In the 221–570 °C temperature range, four processes are observed for ***C2***. In the 221–570 °C temperature range, the release of *bishydeten* and four cyanido molecules is observed with the total weight loss of 33.55% (calc. 33.52%). The most probable thermal decomposition scheme of ***C2*** is given below:

$$[Ni(bishydeten)Au_2(CN)_4] \xrightarrow[-bishydeten,4CN]{221-570^\circ C} NiO + 2Au$$

2.1.4. Antiproliferative effect of *C1*, *C2*, $[Ag(CN)_2]^-$, and $[Au(CN)_2]^-$ against HT-29, HeLa, C6, and Vero cells

In vitro evaluation of the target coordination polymers (***C1*** and ***C2***) and linear ions {$[Ag(CN)_2]^-$ and $[Au(CN)_2]^-$} for their cytotoxic properties was performed by means of BrdU cell proliferation ELISA assays against three cancer cell lines and one noncancerous cell line for the first time. In contrast to the control compound, *5FU*, each coordination polymer significantly inhibited proliferation of HeLa ($P < 0.05$), C6 ($P < 0.05$), HT-29 ($P < 0.05$), and Vero ($P < 0.05$) cells (Figure 1).

It was seen that ***C2*** coordination polymer was five-fold more active than ***C1*** coordination polymer. As shown in Figure 1, each coordination polymer was significantly more antiproliferative against Hela, HT29, and C6 tumor cell lines with lower IC50 concentrations ($P < 0.05$) than the control anticancer drug 5FU. Among

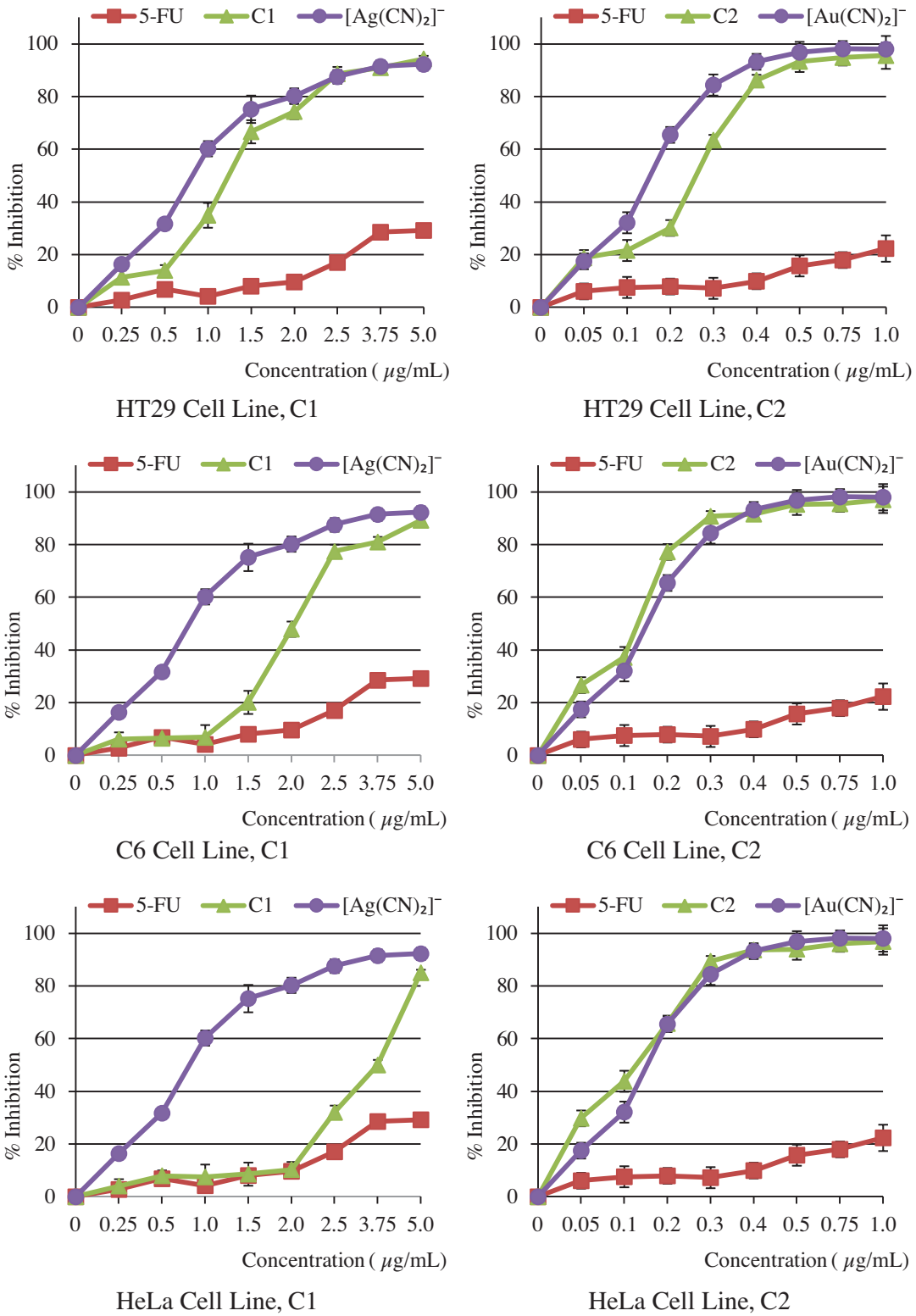

Figure 1. Effects of ***C1***, ***C2***, $[Ag(CN)_2]^-$, and $[Au(CN)_2]^-$ on the proliferation of HeLa, HT-29, C6, and Vero cells. Percent inhibition was reported as mean values ± SEM of three independent assays ($P < 0.05$).

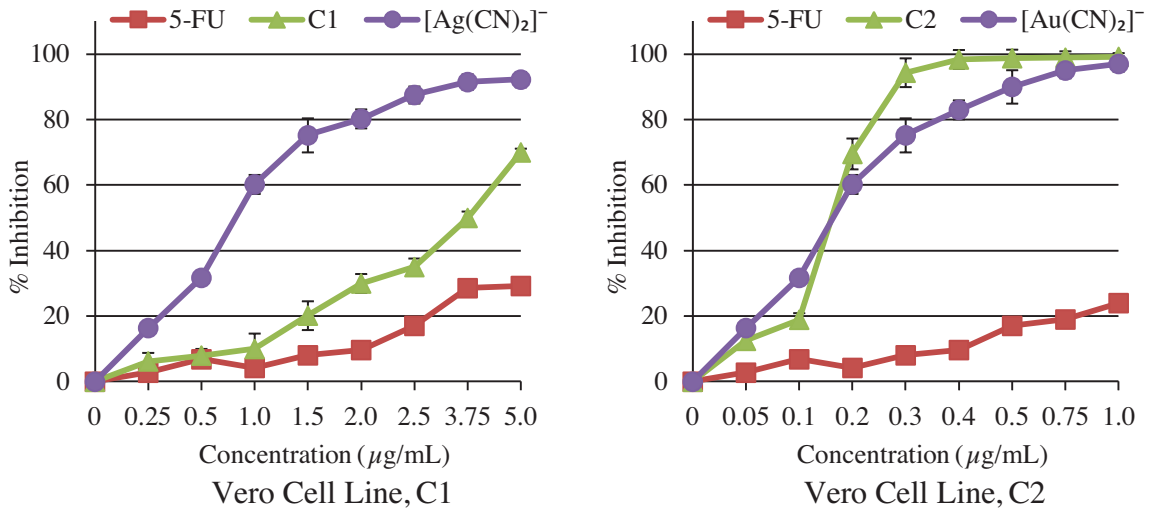

Figure 1. Continued.

all, $[Ag(CN)_2]^-$ and $[Au(CN)_2]^-$ proved more effective than ***C1*** and ***C2*** with IC50 values about 30–35 times lower than 5FU on cells, respectively. IC50 values for ***C1*** and ***C2*** are given in Table 2.

Table 2. IC50 values for ***C1***, ***C2***, 5FU, $[Ag(CN)_2]^-$ and $[Au(CN)_2]^-$.

IC50 μM/L	HeLa	HT29	C6	Vero
C1	3.40	2.40	2.59	2.54
$[Ag(CN)_2]^-$	1.54	1.56	1.53	1.69
5FU	54.28	50.89	42.82	53.62
C2	0.24	0.23	0.34	0.31
$[Au(CN)_2]^-$	0.14	0.16	0.17	0.18
5FU	43.17	34.97	42.37	38.91

2.1.5. Cytotoxic activity of *C1*, *C2*, $[Ag(CN)_2]^-$, and $[Au(CN)_2]^-$ on HT-29, HeLa, and C6 cells

The in vitro cytotoxic activities of ***C1***, ***C2***, $[Ag(CN)_2]^-$, and $[Au(CN)_2]^-$ were evaluated on HeLa, HT29, C6, and Vero cell lines using a lactate dehydrogenase assay (Figure 2).

The results showed that cytotoxicity of each coordination polymer was closed to cytotoxicity of 5FU, except $[Ag(CN)_2]^-$ and $[Au(CN)_2]^-$, at their IC50 concentrations on the cells tested. Results of the LDH assay are expressed in terms of % cytotoxicity values and presented in Figure 2. Each coordination polymer exhibited the same cytotoxic activity as 5FU at IC50 concentration against any of the four cell lines. However, $[Ag(CN)_2]^-$ and $[Au(CN)_2]^-$ were more cytotoxic (% cytotoxicity $\approx$ 55%–98%) than 5FU with 15%–20% cytotoxicity values. The antiproliferative activity levels of coordination polymers and $[Ag(CN)_2]^-$ and $[Au(CN)_2]^-$ on the cell lines tested were almost the same (Figure 1). However, the cytotoxicity of complexes was significantly lower than that of ligands alone ($P < 0.05$) (Figure 2), indicating their high antiproliferative potential with low cytotoxicity.

2.1.6. Apoptosis assay (TUNEL assay)

To investigate whether ***C1*** and ***C2*** induced inhibition of cell proliferation was associated with cell apoptosis, a TUNEL assay was performed to detect apoptotic changes. As shown in Figure 3, ***C1*** and ***C2*** treated HT29

cells showed green fluorescence, indicating fragmented DNA in apoptotic cells, whereas the DMSO control was negative for the staining.

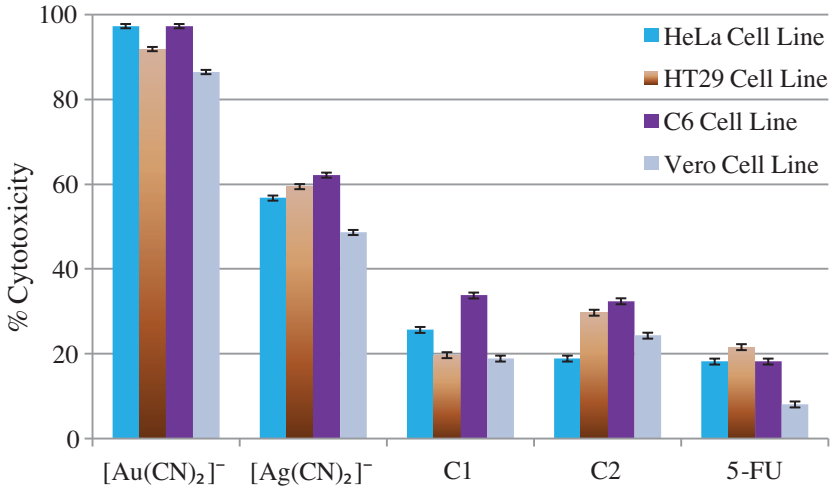

Figure 2. Cytotoxic activity of ***C1***, ***C2***, $[Ag(CN)_2]^-$, and $[Au(CN)_2]^-$ on HeLa, HT29, C6, and Vero cells. The % cytotoxicity of ***C1***, ***C2***, and *5FU* values ranged from 15% to 25%, and % cytotoxicity of $[Ag(CN)_2]^-$ and $[Au(CN)_2]^-$ values approximately 55%–98%. $[Ag(CN)_2]^-$ and $[Au(CN)_2]^-$ were the most cytotoxic compounds ($P < 0.05$) tested against all cell lines. Percent cytotoxicity was reported as mean values ± SDs of three independent assays.

2.1.7. Determination of apoptotic potential of *C1* and *C2*

In the present study, to test whether the mechanism of antiproliferative and cytotoxic activity of ***C1*** and ***C2*** involves apoptosis, we tested the DNA fragmentation potential of ***C1*** and ***C2*** on HeLa, HT29, and C6 cells. The results showed that both coordination polymers caused fragmentation of DNA, indicating that they act by inducing apoptosis (Figure 4).

2.1.8. The effect of *C1* and *C2* on HeLa cell migration

Migration capacity is an important characteristic for cancer. It is strongly expressed that the migration process appears an excellent new target for chemotherapy. Indeed, migrating cancer cells are resistant to apoptosis and it is still the principal target for anticancer drugs. That is, while reducing the levels of migration in apoptosis-resistant cancer cells, the levels of sensitivity to apoptosis in cancer cells increase. ***C1*** and ***C2*** at IC50 concentrations showed a suppressive effect on the migration of the HeLa cell line in a time-dependent manner (Figure 5). It is suggested that ***C1*** and ***C2*** have antimetastatic potential.

2.1.9. Analysis of inhibition of DNA topoisomerase I

DNA topoisomerase I is a nuclear enzyme that plays essential roles in controlling the topological state of DNA to facilitate and remove barriers for vital cellular functions including DNA replication and repair. Therefore, DNA topoisomerase I is an important target of approved anticancer agents. It is found that only ***C1*** at IC50 concentration inhibited the activity of recombinant human DNA topoisomerase I as a positive control, camptothecin (Figure 6). This result may indicate that the compound inhibits cell proliferation by the suppression of DNA topoisomerase I action during replication.

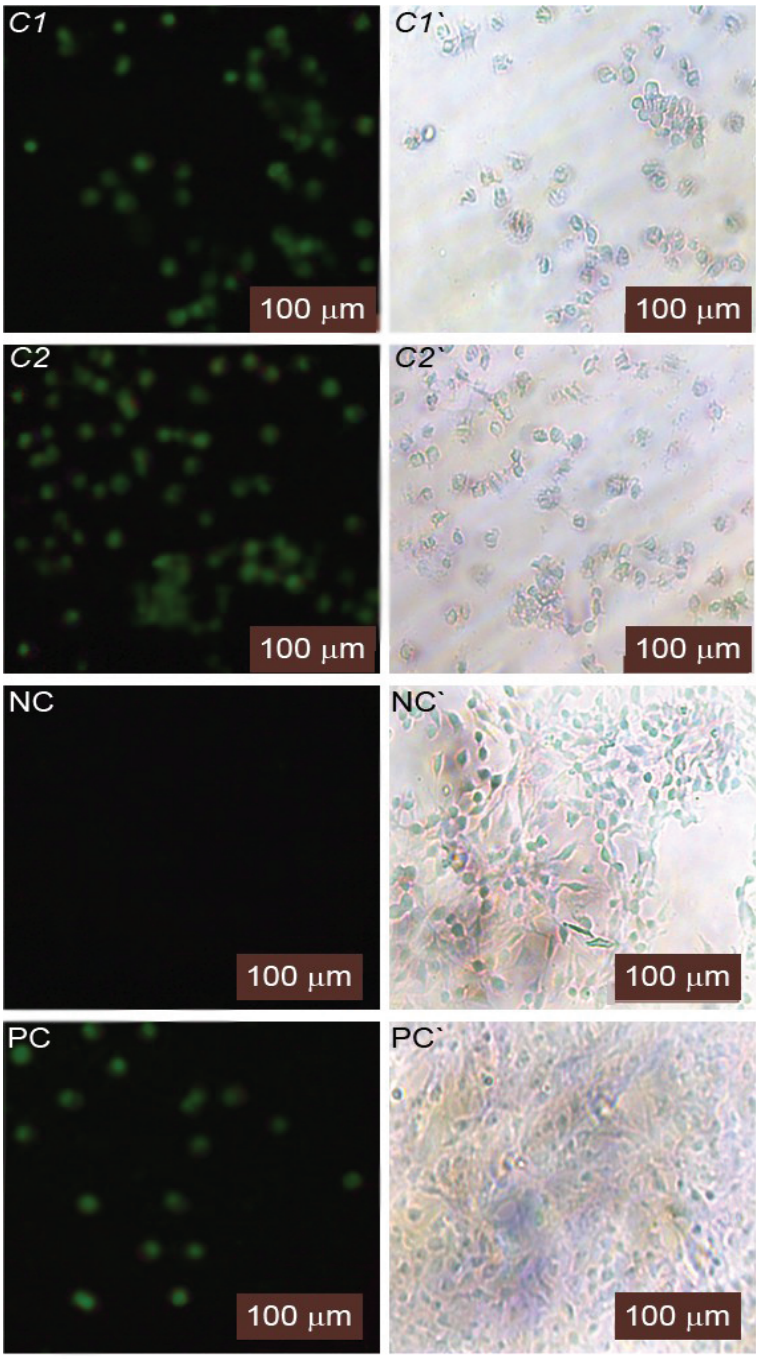

Figure 3. Fluorescence and phase-contrast images of the HT29 cancer cell line examined by TUNEL assay. TUNEL-positive cell nuclei in brilliant green were observed under a fluorescence (***C1***, ***C2***, NC, and PC) and phase-contrast microscope (***C1′***, ***C2′***, NC′, and PC′). ***C1*** and ***C2*** treatment with IC50 induced a significant enhancement of apoptotic cells in contrast to the control group (NC: Negative control, PC: Positive control).

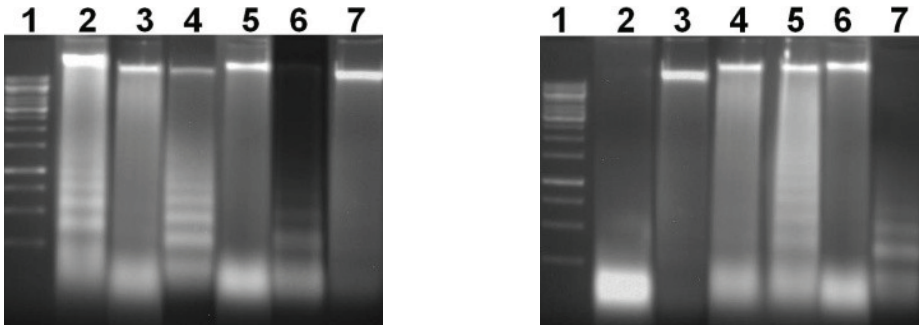

Figure 4. A representative result showing effects of ***C1*** and ***C2*** on internucleosomal DNA fragmentation in cancer cell lines. **A)** Lane 1: DNA standard; Lane 2: HT29 + ***C1***; Lane 3: HT29 Control; Lane 4: C6 + ***C1***; Lane 5: C6 Control; Lane 6: HeLa + C1; Lane 7: HeLa Control. **B)** Lane 1: DNA standard; Lane 2: HeLa + ***C2***; Lane 3: HeLa Control; Lane 4: HT29 Control; Lane 5: HT29 + ***C2***; Lane 6: C6 Control; Lane 7: C6 + ***C2***.

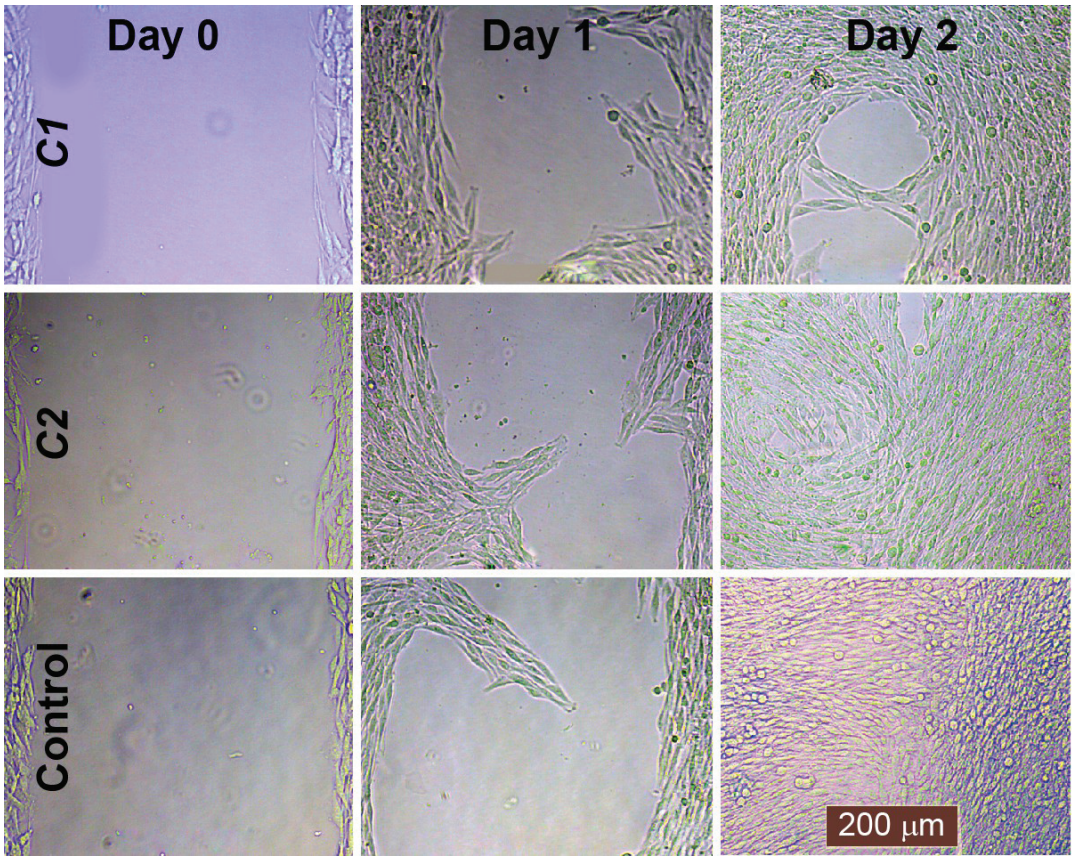

Figure 5. Effect of ***C1*** and ***C2*** on HeLa cell line migration. The speed of cell closure was photographed 0, 1, and 2 days after incubation using a phase contrast microscope (Leica DMIL, Germany) until complete cell closure was observed in the untreated control.

2.1.10. The effect of *C1* and *C2* on the morphology of HeLa, HT29, and C6 cells

The effect of ***C1*** and ***C2*** on the morphology of HeLa, HT29, and C6 cells was visualized (Figure 7).

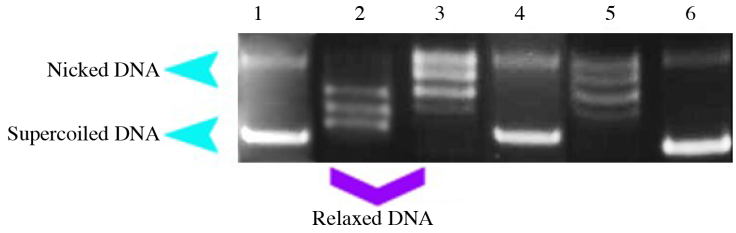

Figure 6. Inhibition of recombinant human topoisomerase I relaxation activity by ***C1*** and ***C2***. Lane 1: Supercoiled marker DNA; Lane 2: Relaxed marker DNA; Lane 3: Negative control (Supercoiled DNA + Topo I); Lane 4: Positive control (Supercoiled DNA + Topo I + Camptothecin); Lane 5: Supercoiled DNA + Topo I + ***C2***; Lane 6: Supercoiled DNA + Topo I + ***C1***.

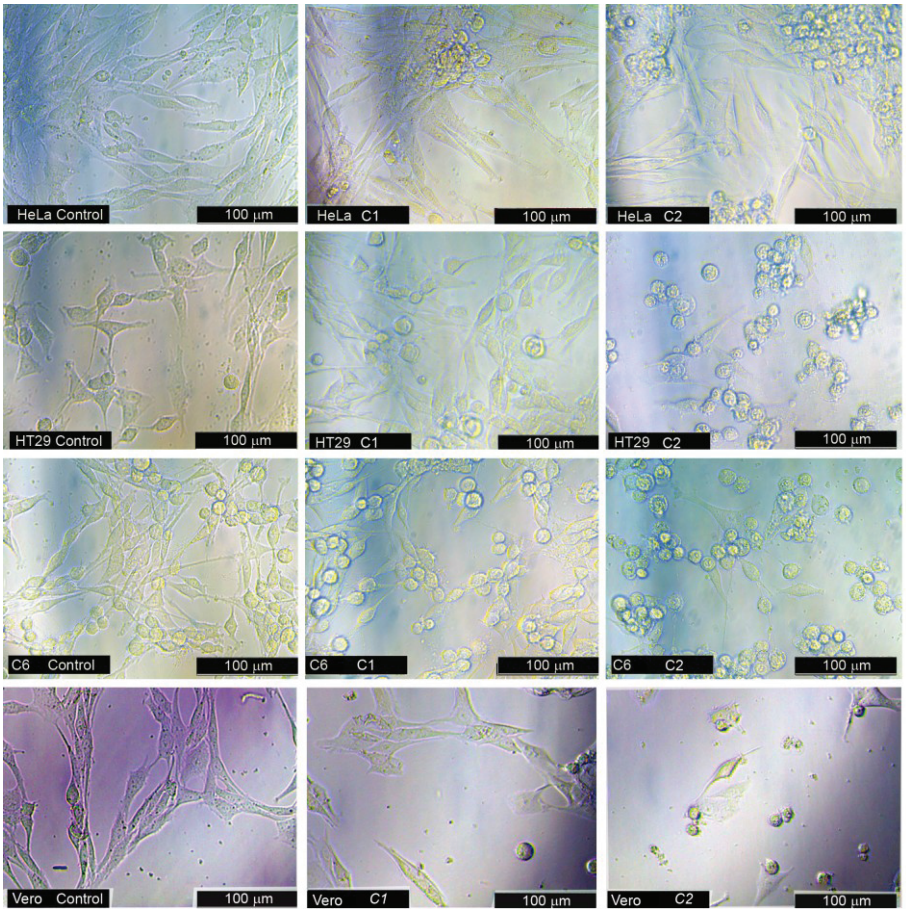

Figure 7. The effect of ***C1*** and ***C2*** on the morphology of HeLa, HT29, C6, and Vero cells. Exponentially growing cells were incubated with IC50 concentrations of ***C1*** and ***C2*** at 37 °C overnight and visualized by digital camera attached inverted microscope (Leica IL10, Germany). DMSO treated cells as controls. All scales 100 μM.

The compounds clearly inhibited the elongation and growth of the cells in culture. All cells were very weakly attached to the surface of the culture plate and became globular upon treatment. C6 and HT29 cells lost their fibroblast-like appearance and HT29 cells clumped together. Apoptotic HeLa, HT29, C6, and Vero cells also had cytoplasmic blebs and shrinkage, and overall decreases in cell volume as apoptotic indicators confirmed by May–Grunwald–Giemsa stain (Figure 8).

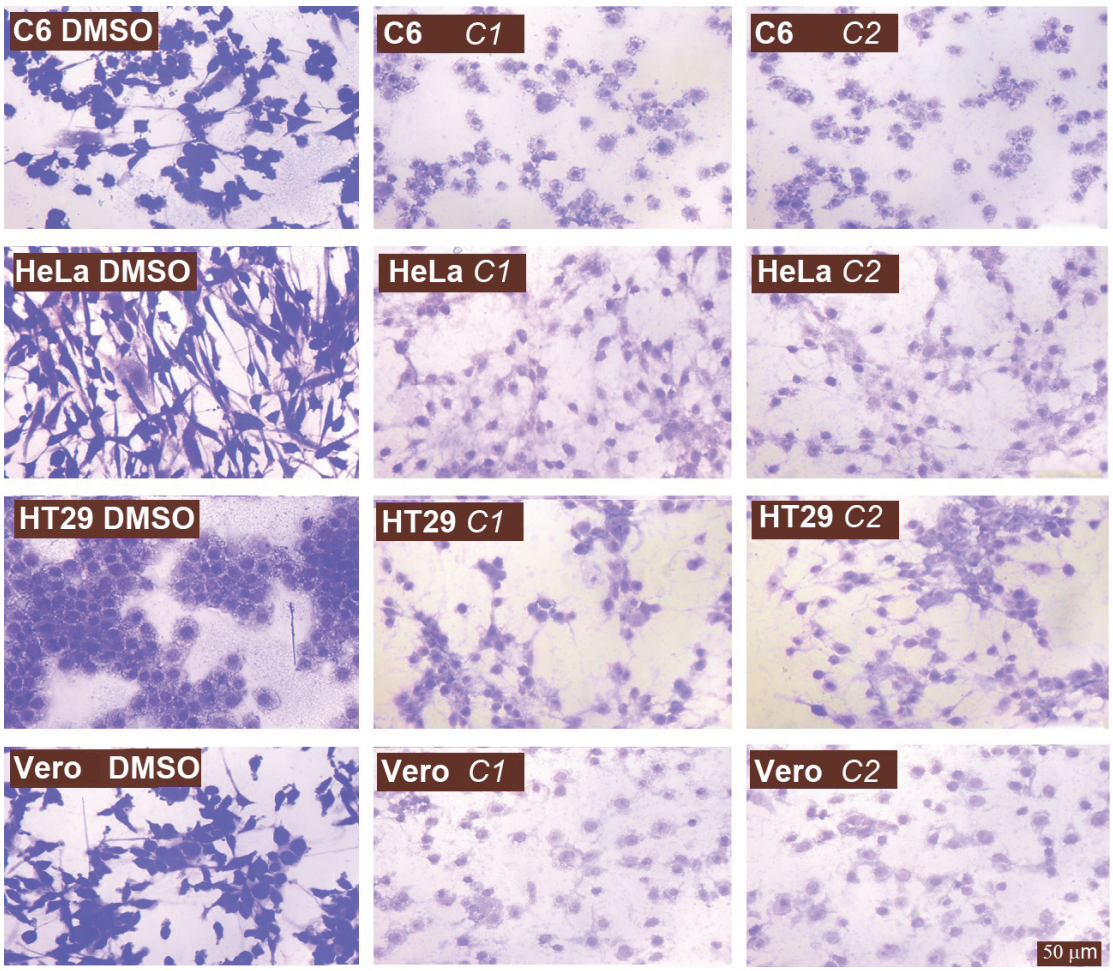

Figure 8. Representative phase contrast microscope (Leica DMIL, Germany) images of May–Grunwald–Giemsa stained cells cultures showing increased apoptotic body treatment cultures, as compared to nontreatment controls.

2.2. Discussion

The present study focused on the development of new metallodrugs against cancer by a biological approach. These innovative metallodrugs may act as recognition biomolecules by targeting specific proteins, RNA, or DNA.[25,26] The metal complexes include coordination compounds that offer quite diverse structural chemistry when targeting biomacromolecules that control or sustain cell growth and survival. Examples of such metal complexes include the ruthenium-based compounds NAMI-A (currently in phase I/II trials) and NKP-1339 (currently in phase I/IIa trials), and the gallium complex KP-46 (currently in phase I/IIa trials).[27]

Silver and gold complexes are extensively studied for their general applications in medicine. The anticancer activity of silver and gold compounds has already been reported in the literature.[28–33] In the present study, the anticancer potential, cytotoxic activity, and mechanisms of action of newly synthesized metal complexes ***C1*** and ***C2*** were investigated on several tumor cell lines, such as HeLa, HT29, and C6. The reason we chose these tumor cell lines was the higher incidence, prevalence, and mortality of cervical, colon, and brain cancers in the world. The results of the cell proliferation assay showed that the Ag(I) and Au(I) compounds were significantly more antiproliferative than 5FU (Figure 1) against the cell lines, indicating their anticancer potential, as in previous studies.[34–38]

It is known that cisplatin-like metallodrugs inhibit cell proliferation by binding to cell DNA; however, it is not clear yet whether ***C1*** and ***C2*** bind to cell DNA. In addition, ***C1*** and **C2** complexes were as cytotoxic as 5FU against all tumor cell lines tested at their IC50 concentrations (Figure 2). It is very clear that the cytotoxicity of ***C1*** and ***C2*** against nontumorigenic Vero cells was significantly low. To sum up, each coordination polymer showed significantly low cytotoxicity ($P < 0.05$) compared to $[Ag(CN)_2]^-$ and $[Au(CN)_2]^-$ alone, indicating that the complex structure of ***C1*** and ***C2*** decreases cytotoxicity without reducing their antiproliferative potential (Figure 2). It is suggested that ***C1*** and ***C2*** may have cytostatic potential rather than cytotoxicity, whereas free $[Ag(CN)_2]^-$ and $[Au(CN)_2]^-$ clearly have more cytotoxic activity. That is, these coordination polymers are better candidates for potential anticancer therapy for cancerous diseases. Widespread research has been undertaken to determine the antiproliferative and cytotoxic effects of Ag and Au complexes and is consistent with this study.[39–41]

In vitro proliferation studies confirmed significant apoptotic activity of Ag(I) and Au(I) complexes, with IC50 values ranging from 0.1 to 2.0 μg/mL HT29 cells. Apoptosis was examined using the terminal deoxynucleotidyl transferase dUTP nick and labeling (TUNEL) method in the HT29 cell line. In vitro studies with TUNEL showed that ***C1*** and ***C2***significantly induced apoptosis (Figure 3). It is known that enhanced antitumor efficacy is associated with increased induction of apoptosis. Therefore, these findings indicated that ***C1*** and ***C2*** inhibited HT29 cancer cell line growth in vitro. As illustrated in Figure 3, ***C1*** and ***C2*** treatment caused a significantly higher ratio of TUNEL-positive apoptotic cells. These results indicated that ***C1*** and ***C2*** have a vigorous anticancer effect on the HT29 cancer cell line and are potent apoptosis-inducing agents in vitro. The Ag(I) and Au(I) complexes caused a dose-dependent induction of apoptosis in cancer cells, primarily through a group of protease-mediated pathways, as suggested by the ability of DNA laddering in coordination-polymer-treated cells. Typical results from cancer cells treated with each compound are shown in Figure 4. These compounds induced the formation of DNA fragmentation in cancer cell lines compared to the control cells (Figure 4). In untreated cells, there was no DNA fragmentation, and intact genomic DNA was situated near the well at the top of the lanes. The appearance of apoptotic morphology and DNA fragmentation may be a result of the binding of compounds to DNA. The migration assay revealed a suppressive effect of ***C1*** and ***C2*** treatment on HeLa cell migration ability in a time-dependent manner (Figure 5). After exposure to IC50 concentrations of ***C1*** and ***C2***, there were great differences in the migration rate of both cell lines compared with the untreated control (Figure 5). These results show that ***C1*** and ***C2*** were more effective in suppressing the migration capacity of cancer cells.

C1 and ***C2*** may also cause modulated cell death and apoptotic stress resulting from cell migration, which are both processes that are intimately involved in cancer progression. ***C1*** and ***C2*** can restrict the levels of migration of HeLa cancer cells, and they should therefore be used in association with anticancer drugs to fight cancer. ***C1*** and ***C2*** were found to inhibit tumor cell migration with low cytotoxicity. Most cancer cells are defined by a more robust invasive potential than normal cells. A successful cancer treatment is required to suppress cancer cell proliferation and migration potential, since cancer cells escaping from the primary tumor site colonize different metastatic sites. This study showed for the first time that ***C1*** and ***C2*** are able to reduce HeLa cell migration and most likely decrease the expression of surface-expressed ligands such as cellular adhesion molecules.

DNA topoisomerase I has been identified as an important antitumor target because of its essential physiological functions of regulating DNA topology during DNA replication and recombination. Topoisomerase inhibitor agents are now used in routine clinical practice (camptosar, irinotecan, and topotecan). There has

been continuous interest in studying and developing new antitopoisomerase agents.[42–44] The effects of ***C1*** and ***C2*** on topoisomerase I-mediated supercoiled pHOT1 relaxation were investigated. The results revealed that the IC50 concentration of ***C1*** inhibited almost all of the relaxation activity of topoisomerase I, whereas the IC50 concentration of ***C2*** failed to show any effect on topoisomerase I (Figure 6). Hence, based on this initial experiment, ***C1*** was selected for further preclinical development owing to its potent antitopoisomerase feature in vitro.

The morphology of cells was investigated using phase-contrast microscopy. As shown in Figure 7, obvious morphological changes were observed in the treated cells in a dose-dependent manner compared to the untreated cells. Each cell line exposed to the compounds exhibited cytoplasmic blebs, shrinkage, anomalous globular structure, and the appearance of apoptotic bodies as apoptotic indicators (Figure 7). This was consistent with the results of the BrdU cell proliferation ELISA assay and DNA laddering test. Moreover, all cell lines treated with ***C1*** and ***C2*** showed apoptotic indicators, which was confirmed by May–Grunwald–Giemsa stain (Figure 8). These results were somewhat similar to those of previous studies by Hall et al.,[45] Rackham et al.,[46] Thati et al.,[47] Wang et al.,[48] Wang et al.,[49] and Zhu et al.[50] Thus, based on observations in the literature, the appearance of cell lines treated with ***C1*** and ***C2*** clearly indicated the antiproliferative and low-cytotoxic effect of these complexes. Moreover, the results of DNA fragmentation assays and TUNEL assay indicate that these novel complexes may inhibit cell proliferation through the induction of apoptosis.

To sum up, we have demonstrated for the first time that the strong apoptosis inducers ***C1*** and ***C2*** possess vigorous inhibitory effects on cancer cell lines in vitro. Based on our results, it is suggested that both complexes are potentially valuable anticancer drug candidates and are suitable for further pharmacological testing. We think that there is a great need for large and well-designed anticancer activity studies of new anticancer agents built from parent compounds ***C1*** and ***C2*** with better solubility in biological fluid and less toxicity**.**

3. Experimental

3.1. Preparations

$AgNO_3$, KCN, $NiCl_2.6H_2O$, $K[Au(CN)_2]$, $Ni(ClO_4)_2.6H_2O$, 2,2′-(ethylenedioxy) bis(ethylamine) (*edbea*), and N,N'-bis(2-hydroxyethyl)ethylenediamine (*bishydeten*) were used as received.

3.2. Synthesis of $[Ni(edbea)Ag_3(CN)_5]_n$ (*C1*)

The solid KCN (153 mg, 1.175 mmol) was added to water:ethanol (1:3; 20 mL) solution of $AgNO_3$ (200 mg, 1.177 mmol) and shortly after clear $K[Ag(CN)_2]$ solution was formed. Then $NiCl_2.6H_2O$ (280 mg, 1.177 mmol) was added to the solution of $K[Ag(CN)_2]$, resulting in a light blue slurry. When *edbea* (350 mg, 1.180 mmol) was added to the obtained slurry under continuous stirring, a pink precipitate was formed within 5 min. The product was filtered off, washed with water and alcohol, and then dried in air. Yield: 70%. Anal. Calc. (%) for $C_{11}H_{16}N_7O_2Ag_3Ni$ (***C1***): *C* 20.00, *H* 2.44, *N* 14.84, found: *C* 19.75, *H* 2.56, *N* 14.45. IR spectra (KBr disk; cm^{-1}) 3342, 3276 [υ_{NH}]; 2944, 2906, 2865 [υ_{CH}]; 2161[$\upsilon_{C\equiv N}$]; 1592 [δ_{NH}]; 1101, 1031 [υ_{CO}].

3.3. Synthesis of $[Ni(bishydeten)Au_2(CN)_4]_n$ (*C2*)

$K[Au(CN)_2]$ (0.506 mmol, 0.146 g) was added to a water:ethanol (1:1; 20 mL) solution and $Ni(ClO_4)_2.6H_2O$ (0.506 mmol, 0.185 g) was slowly added to the resulting blue suspension mixture. An ethanolic solution (15 mL) of *bishydeten* (0.507 mmol, 0.075 g) was then added and a pink precipitate was formed within 5 min. The

pink precipitate formed was filtered, washed with water and ethanol, and dried in air. Yield: 35%. Anal. Calc. (%) for $C_{10}H_{16}N_6O_2NiAu_2$ ***(C2)***: *C* 17.04, *H* 2.29, *N* 11.92, found: *C* 17.44, *H* 2.54, *N* 11.57. IR spectra (KBr disk cm^{-1}) 3446 [υ_{OH}]; 3255, 3220 [υ_{NH}]; 2938, 2881 [υ_{CH}]; 2194, 2173, 2150 [$\upsilon_{C\equiv N}$]; 1596 [δ_{NH}]; 1068[υ_{CO}].

3.4. Cell culture

C6, HT29, HeLa, and Vero cell lines were maintained in Dulbecco's modified eagle's medium (DMEM, Sigma) supplemented with 10% (v/v) fetal bovine serum (Sigma, Germany) and PenStrep solution (10,000 U/10 mg) (Sigma, Germany) (ATCC, American Type Culture Collection).[51,52] At confluence, cells were detached from the flasks using 4 mL of trypsin-EDTA (Sigma, Germany) and centrifuged, and the cell pellet was resuspended with 4 mL of supplemented DMEM.

3.5. Cell proliferation assay (CPA)

A cell suspension containing 3×10^3 cells in 100 μL was pipeted into the wells of 96-well cell culture plates (COSTAR, Corning, USA). The test compounds (***C1***, ***C2***, $[Ag(CN)_2]^-$, and $[Au(CN)_2]^-$) and a positive control compound (5 fluorouracil, 5FU) were dissolved in sterile DMSO. The amount of DMSO was adjusted to 0.5% maximum. The cells were treated with ***C1***, $[Ag(CN)_2]^-$, and 5FU at final concentrations of 0.25, 0.50, 1.00, 1.50, 2.00, 2.50, 3.75, and 5.00 μg/mL and were treated with ***C2***, $[Au(CN)_2]^-$, and 5FU at final concentrations of 0.05, 0.1, 0.2, 0.3, 0.4, 0.5, 0.75, and 1.00 μg/mL. Cell controls and solvent controls were treated with supplemented DMEM and sterile DMSO, respectively. The final volume of the wells was adjusted to 200 μL with supplemented DMEM.

The cells were then incubated at 37 °C with 5% CO_2 overnight. The antiproliferative activity of the compounds was determined using a BrdU Cell proliferation ELISA kit according to the manufacturer's protocol (Roche, USA) for a calorimetric immunoassay based on BrdU incorporation into the cellular DNA. Briefly, cells were exposed to BrdU labeling reagent for 4 h, followed by fixation in FixDenat solution for 30 min at room temperature. Then cells were cultured with a 1:100 dilution of anti-BrdU-POD for 1 h and 30 min at room temperature. Substrate solution was added to each well, and BrdU incorporation was measured at 450–650 nm using a microplate reader (Rayto, China). Each experiment was repeated at least three times for each cell line.

3.6. Calculation of IC50 and % inhibition

IC50 represents the concentration of an agent that is required for 50% inhibition in vitro. The half maximal inhibitory concentration (IC50) of the test and control compounds was calculated using XLfit5 software (IDBS) and expressed in μM/L at 95% confidence intervals. The CPA assay results were reported as the percent inhibition of the test and control substances. The percent inhibition was calculated according to the following formula: % inhibition = [1 − (Absorbance of Treatments/Absorbance of DMSO) × 100].

3.7. Cytotoxic activity assay

The cytotoxicity of ***C1***, ***C2***, $[Ag(CN)_2]^-$, $[Au(CN)_2]^-$, and 5FU on C6, HT29, HeLa, and Vero cells was determined using a Lactate Dehydrogenase (LDH) Cytotoxicity Detection Kit (Roche, USA) based on the measurement of LDH activity released from the cytosol of damaged cells into the supernatant according to the manufacturer's instructions; 3×10^4 cells in 100 μL were seeded into 96-well microtiter plates as triplicates

and treated with IC50 concentrations of ***C1***, ***C2***, $[Ag(CN)_2]^-$, $[Au(CN)_2]^-$, and 5FU as described above at 37 °C with 5% CO_2 overnight. LDH activity was determined by measuring absorbance at 492–630 nm using a microplate reader.

3.8. Terminal deoxynucleotidyl transferase dUTP nick end labeling (TUNEL) assay

In vitro detection of apoptosis was assessed using a TUNEL assay kit (Roche, Germany) according to the manufacturer's protocol. HT29 cell lines (30,000 cells/well) were placed in a poly-L-lysine covered chamber slide. The cells were treated with IC50 concentrations of ***C1*** and ***C2*** and left for 24 h of incubation. There were two controls for this assay: one was a positive control that had DNase-1 treatment and the other was a negative control that had no terminal deoxynucleotidyl transferase (TdT).

When the incubation time was over, the chamber was removed from the slide and washed with DPBS to remove the medium and unattached cells. All of the incubation and washing steps were done in a plastic jar. The slides were gently washed with DPBS, and for fixation 4% paraformaldehyde in DPBS at pH 7.4 was freshly prepared and added to the slides for 60 min at room temperature. Following incubation, the slides were washed twice with DPBS. The cells were blocked with freshly prepared 3% H_2O_2 in methanol for 10 min at room temperature. Following incubation, the slides were washed twice with DPBS.

The cells were permeabilized by prechilled 0.1% Triton X-100 and freshly prepared 0.1% sodium citrate in water and then incubated for 2 min on ice. All the slides were washed with DPBS twice for 5 min each. At this point, in order to prepare a DNase I enzyme-treated positive control, 100 μL of DNase-1 buffer was added to the slide, which was incubated at room temperature for 10 min. Fixative cells were transferred into a TUNEL reaction mixture (50 μL/section) containing TdT and fluorescein-dUTP. Intracellular DNA fragments were then labeled by exposing the cells to TUNEL reaction mixture for 1 h at 37 °C in a humidified atmosphere and protected from light. After washing with DPBS twice, cells positive for apoptosis showed a green fluorescent signal and were visualized by a Leica fluorescent microscope (Leica DMIL LED fluo, Germany).

3.9. Analysis of DNA fragmentation (DNA laddering test)

DNA fragmentation effect of the test compounds was measured according to the method of Gong et al.[53] with some modifications. Briefly, 7.5×10^5 cells were seeded into 25-cm^2 culture flasks, and treated with IC50 concentrations of ***C1*** and ***C2*** at 37 °C with 5% CO_2 for overnight. Treated cells were harvested using a sterile plastic scraper, transferred to a 15-mL sterile Falcon tube, washed with 1 mL of sterile DPBS, and pelleted by spinning at 1500 $\times g$ for 5 min. The cell pellet was resuspended with 200 μL of ice cold DPBS by gently pipeting, fixed with 5 mL of ice cold 70% ethanol, vortexed briefly, and incubated at –20 °C for 24 h. The cells were centrifuged at 1500 $\times g$ for 5 min, the supernatant was removed, and the remaining ethanol removed by air drying. The cell pellet was resuspended in 50 μL of phosphate-citrate buffer (consisting of 192 parts of 0.2 M Na_2HPO_4 and 8 parts of 0.1 M citric acid, pH 7.8), incubated at 37 °C for 30 min in a shaker incubator, and centrifuged at 1500 $\times g$ for 5 min. Then 40 μL of supernatant was transferred to a 1.5-mL microcentrifuge tube, mixed with 5 μL of Tween20 solution (0.25% in ddH_2O) and 5 μL of RNase A solution, and incubated at 37 °C for 30 min in a shaker incubator. Next, 5 μL of proteinase K was added to each tube and incubated at 37 °C for 10 min. Finally, the entire content of the microcentrifuge tube was mixed with 4 μL of 6X loading buffer, loaded to 1.5% agarose gel containing 0.5 μg/mL ethidium bromide, and electrophoresed at 200 mA for 40 min. DNA fragmentation in the gels was visualized using a gel documentation system (UVP, England).

3.10. Cell migration assay

The migration capability of cells was measured using the migration assay. Briefly, a culture insert (ibidi GmbH, Germany) consisting of two reservoirs separated by a 500 μm thick wall was placed on a 35-mm petri dish, and equal numbers of HeLa cells (3.5×10^4 HeLa cells in 70 μL of DMEM medium) were seeded into the two reservoirs of the same insert and allowed to grow to 90%–95% confluence, in order to generate a 500-μm gap between the two cell populations. Subsequent to cell growth, the insert was gently removed and 2 mL of cell culture medium was added, then treated with IC50 concentrations of ***C1*** and ***C2***, and shortly after incubated overnight at 37 °C with 5% CO_2. The speed of cell closure was photographed 0, 1, and 2 days after incubation using a phase contrast microscope (Leica DMIL, Germany) until complete cell closure was observed in the untreated control.

3.11. DNA topoisomerase I inhibition assay

The DNA topoisomerase I inhibitory activities of ***C1*** and ***C2*** were evaluated using a cell-free topoisomerase I assay kit (TopoGen, USA). The principle of the assay is to measure the conversion of supercoiled pHOT1 plasmid DNA to its relaxed form in the presence of DNA topoisomerase I alone and with test compounds. The supercoiled substrate (pHOT1 plasmid DNA) and its relaxed product can easily be distinguished in agarose gel, because the relaxed isomers migrate more slowly than the supercoiled isomer. In brief, 20 μL of reaction mixture containing 1 μL of plasmid pHOT1 DNA in relaxation buffer was incubated with 2 U recombinant human topoisomerase I enzyme in the presence of IC50 concentrations of ***C1***, ***C2***, or camptothecin as positive control. The reactions were carried out at 37 °C for 30 min and then terminated by the addition of stop solution. After the termination, the sample was analyzed using 1% agarose gel at 4 V/cm for 60 min. After electrophoresis, DNA bands were stained with ethidium bromide (EtdBr) (1 mg/mL) solution and photographed through a gel imaging system (UVP BioSpectrum, Germany).

3.12. Cell staining and imaging

Cells were seeded in 96-well plates at a density of 5000 cells per well and allowed 24 h for attachment. Using previously established IC50 doses of ***C1*** and ***C2*** treatment was performed for 24 h, during which morphology changes were assessed by phase contrast microscopy. Images of vehicle (DMSO), ***C1***, and ***C2*** treated cells were taken at the end of experimental period using a digital camera attached inverted microscope (Leica IL10, Germany). Additionally, cell lines were grown in chamber slides (Ibidi, Germany) at a concentration of 15,000 cells per well and treatment with ***C1*** and ***C2***. At the end of incubation, the cells were air dried and stained with May–Grunwald–Giemsa. Stained cells were analyzed under a light microscope.

4. Statistical analysis

The statistical significance of differences was determined by one-way analysis of variance (one-way ANOVA) tests. Post hoc analyses of group differences were performed using the Tukey test, and the levels of probability were noted. SPSS for Windows was used for the statistical analyses. The results are reported as the mean values ± SEM of three independent assays, and differences between groups were considered to be significant at $P < 0.05$.

Acknowledgment

This study was supported by TÜBİTAK through project no. 112T696

References

1. Ávalos Fúnez, A.; Isabel Haza, A.; Mateo, D.; Morales P. *Toxicol. Mech. Methods.* **2013**, *23*, 153–160.
2. Berners-Price, S. J.; Johnson, R. K.; Giovenella, A. J.; Faucette, L. F.; Mirabelli, C. K.; Sadler, P. J. *J. Inorg. Biochem.* **1998**, *33*, 285–295.
3. Boulikas, T.; Pantos, A.; Bellis, E.; Christofis, P. *Cancer Therapy.* **2007**, *5*, 537–583.
4. Ott, I.; Gust, R. *Arch. Pharm. Chem. Life Sci.* **2007**, *340*, 117–126.
5. Kelland, L. *Nat. Rev. Cancer* **2007**, *7*, 573.
6. Kriel, F. H.; Coates, J. *S. Afr. J. Chem.* **2012**, *65*, 271–279.
7. Zachariadis, P. C.; Hadjikakou, S. K.; Hadjiliadis, N.; Skoulika, S.; Michaelides, A.; Balzarini, J.; De Clercq, E. *Eur. J. Inorg. Chem.* **2004**, *7*, 1420–1426.
8. El-Din, H. E. S.; Ahmed, S. S.; Ahmed, S. B. E. *Eur. J. Med. Chem.* **2011**, *46*, 5370–5378.
9. Liu, J. J.; Galettis, P.; Farr, A.; Maharaj, L.; Samarasinha, H.; McGechan, A. C.; Baguley, B. C.; Bowen, R. J.; Berners-Price, S. J.; McKeage, M. J. *J. Inorg. Biochem.* **2008**, *102*, 303–310.
10. Sun, R. W. Y.; Che, C. M. *Coord. Chem. Rev.* **2009**, *253*, 1682–1691.
11. Chabner, A.; Lynch, T. J.; Longo, D. L.; Yılmaz, B. D. *Harrison Onkoloji El Kitabı*; Nobel Tıp Kitapevleri: İstanbul, Turkey, 2009.
12. Dhar, S.; Lippard, S. J. *Proc. Natl. Acad. Sci.* **2009**, *106*, 22199–22204.
13. Wang, C. H.; Shih, W. C.; Chang, H. C.; Kuo, Y. Y.; Hung, W. C.; Ong, T. G.; Li, W. S. *J. Med. Chem.* **2011**, *28*, 5245–5249.
14. Thurston, D. E. *Chemistry and Pharmacology of Anticancer Drugs*; CRC Press, Taylor & Francis Group: Boca Raton, FL, USA, 2007.
15. Karadağ, A.; Keskin, G. A.; Yılmaz, V. T.; Yerli, Y.; Şahin, E. *Polyhedron* **2014**, *78*, 24–30.
16. Korkmaz, N. PhD, Department of Chemistry, University of Gaziosmanpaşa, Tokat, 2014.
17. Şenocak, A.; Karadağ, A.; Yerli, Y.; Andaç, Ö.; Şahin, E. *J. Inorg. Organomet. Polym.* **2010**, *20*, 628–635.
18. Şenocak, A.; Karadağ, A.; Şahin, E. *J. Inorg. Organomet. Polym.* **2013**, 1008–1014.
19. Şenocak, A.; Karadağ, A.; Yerli, Y.; Gürbüz, N.; Özdemir, İ.; Şahin, E. *Polyhedron* **2013**, *49*, 50–60.
20. Şenocak, A.; Karadağ, A.; Şahin, E.; Yerli, Y. *J. Inorg. Organomet. Polym.* **2011**, *21*, 438–449.
21. Nakamato, K. *Infrared and Raman Spectra of Inorganic and Coordination Compounds Part B*; John Wiley & Sons: Hoboken, NJ, USA, 2009.
22. Yılmaz, V. T.; Karadağ, A. *Thermochim. Acta.* **2000**, *348*, 121–127.
23. Yakupoğlu, F.; Karadağ, A.; Şekerci, M. *J. Therm. Anal. Cal.* **2006**, *86*, 727–731.
24. Karadağ, A. *Z. Kristallogr.* **2007**, *222*, 39–45.
25. Avendaño, C.; Menéndez, J. C. *Medicinal Chemistry of Anticancer Drugs*; Elsevier BV: Amsterdam, the Netherlands, 2008.
26. Gielen, M.; Tiekink, E. R. T. *Metallotherapeutic Drugs and Metal-Based Diagnostic Agents—the Use of Metals in Medicine*; John Wiley & Sons: West Sussex, UK, 2005.
27. Roche, V. F. In *Foye's Principles of Medicinal Chemistry*; Williams, D. A.; Lemke, T., Eds. Lippincott Williams & Wilkins: Baltimore, MD, USA, 2002, pp. 1147–1192.

28. Batarseh, K. I. *Curr. Med. Chem.* **2013**, *20*, 2363–2373.
29. Caruso, F.; Villa, R.; Rossi, M.; Pettinari, C.; Paduano, F.; Pennati, M.; Daidone, M. G.; Zaffaroni, N. *Biochem. Pharmacol.* **2007**, *73*, 773–781.
30. Casini, A.; Cinellu, M. A.; Minghetti, G.; Gabbiani, C.; Coronnello, M.; Mini, E.; Messori, L. *J. Med. Chem.* **2006**, *49*, 5524–5531.
31. Cuin, A.; Massabni, A. C.; Pereira, G. A.; Leite, C. Q.; Pavan, F. R.; Sesti-Costa, R.; Heinrich, T. A.; Costa-Neto, C. M. *Biomed. Pharmacother.* **2011**, *65*, 334–338. Gandin, V.; Pellei, M.; Marinelli, M.; Marzano, C.; Dolmella, A.; Giorgetti, M.; Santini, C. J. Inorg. *Biochem.* **2013**, *129*, 135–144.
32. Govender, R.; Phulukdaree, A.; Gengan, R. M.; Anand, K.; Chuturgoon, A. A. *J. Nanobiotechnology* **2013**, *11*, 5.
33. Korany, A.; Ali, M. M.; Abd-Elzaher, K. M. *Int. J. Med. Chem.* **2013**, 1–7.
34. Pettinari, C.; Marchetti, F.; Lupidi, G.; Quassinti, L.; Bramucci, M.; Petrelli, D.; Vitali, L. A.; da Silva, M. F.; Martins, L. M.; Smoleński, P.; et al. *Inorg. Chem.* **2011**, *50*, 11173–11183.
35. Banti, C. N.; Hadjikakou, S. K. *Metallomics* **2013**, *5*, 569–596.
36. Aydın, A.; Korkmaz, N.; Tekin, Ş.; Karadağ, A. *Turk J Biol.* **2014**, *38*, 948–955.
37. Korkmaz, N.; Karadağ, A.; Aydın, A.; Yanar, Y.; Karaman, İ.; Tekin, Ş. *New J. Chem.* **2014**, *38*, 4760.
38. Iqbal, M. A.; Haque, R. A.; Nasri, S. F.; Majid, A. A.; Ahamed, M. B.; Farsi, E.; Fatima, T. *Chem. Cent. J.* **2013**, *1*, 27.
39. Medvetz, D. A.; Hindi, K. M.; Panzner, M. J.; Ditto, A. J.; Yun, Y. H.; Youngs, W. J. *Met. Based Drugs* **2008**, 384010.
40. Monlien, F. J.; Helm, L.; Abou-Hamdam, A.; Merbach, A. E. *Inorg. Chim. Acta* **2002**, *331*, 257–269.
41. Champoux, J. J. *Annu. Rev. Biochem.* **2001**, *70*, 369–413.
42. Prabhakaran, R.; Sivasamy, R.; Angayarkanni, J.; Huang, R.; Kalaivani, P.; Karvembu, R.; Dallemer, F.; Natarajan, K. *Inorg. Chim. Acta* **2011**, *374*, 647–653.
43. Wu, X.; Yalowich, J. C.; Hasinoff, B. B. J. Inorg. *Biochem.* **2011**, *6*, 833–888.
44. Hall, I. H.; Miller, M. C.; West, D. X. *Met. Based Drugs* **1997**, *2*, 89–95.
45. Rackham, O.; Nichols, S. J.; Leedman, P. J.; Berners-Price, S. J.; Filipovska, A. *Biochem. Pharmacol.* **2007**, *74*, 992–1002.
46. Thati, B.; Noble, A.; Creaven, B. S.; Walsh, M.; McCann, M.; Kavanagh, K.; Devereux, M.; Egan, D. A. *Cancer Letters* **2007**, *248*, 321–331.
47. Wang, H. J.; Yang, L.; Yang, H. Y.; Wang, K.; Yao, W. G.; Jiang, K.; Huang, X. L.; Zheng, Z. *J. Inorg. Biochem.* **2010**, *104*, 87–91.
48. Wang, Y.; He, Q. Y.; Sun, R. W.; Che, C. M.; Chiu, J. F. *Eur. J. Pharmacol.* **2007**, *554*, 113–122.
49. Zhu, H. L.; Zhang, X. M.; Liu, X. Y.; Wang, X. J.; Liu, G. F.; Usman, A.; Fun, H. K. *Inorg. Chem. Commun.* **2003**, *6*, 1113–1116.
50. Murphy, A.; Vines, A.; McBean, G. J. *Biochim. Biophys. Acta.* **2009**, *2*, 551–558.
51. Yoshimoto, A. N.; Bernardazzi, C.; Carneiro, A. J. V.; Elia, C. C. S.; Martinusso, C. A.; Ventura, G. M.; Castelo-Branco, M. T. L.; de Souza, H. S. P. *PLoS One* **2012**, *9*, 45332.
52. Gong, J.; Traganos, F.; Darzynkiewicz, Z. *Anal. Biochem.* **1994**, *218*, 314–319.